CHAPTER 3

MAGNETIC FIELD INFLUENCE ON CRYSTALLIZATION, ORIENTATION and CHEMICAL REACTION

This chapter consists of review in recent progress on weak magnetic field influence on chemical reaction and crystallization. How magnetic field improve the crystal quality and liquid crystal orientation in favour of energy useful process. In principle, Lorentz and the magnetization force influence species in solution and free electrons in materials, and magnetic torque is acting on the species having anisotropic magnetic susceptibility. With external magnetic field physical and chemical characteristics of the chemical system can be affected. Magnetic torque from external magnetic field influence viscosity of the system. Weak magnetic field does not fit inside of Hartmann number as significant force of crystallization and orientation of melt or liquid. Focus on possible influence of magnetic field on radical pairing and chemistry of spark discharge gap with experimental results is presented.

3.1 Introduction

Material magnetic properties are divided into 5 classes according to their behavior in a magnetic field: a) Diamagnetic, b) Paramagnetic, c) Ferromagnetic, d) Antiferromagnetic and e) Ferrimagnetic. These classes are magnetic attributes of materials that greatly differ in strength. The spin of electrons in molecules and atoms that the material is composed of interacts with magnetic field which is known as magnetic force or Kelvin force.

Can magnetic field influence non-magnetic materials and substances?

The magnetic field is always coupled to the electric charges and therefore it is logical that it has an action on the non-magnetic materials as well as the magnetic ones. One example is the Hall effect that is production of electron voltage across conducting or

semiconducting material, set across to an electric current in the conductor and to applied magnetic field.

Hall effect is the classic and the quantum integer or the fractional one.(1) The fundamental reason is that the linear momentum changes when the magnetic field is present and hence the kinetic energy too, producing a change in the Hamiltonian operator making appear the Landau levels. The charged particles can only occupy orbits with discrete energy values, The Landau levels are degenerate, with the number of electrons per level directly proportional to the strength of the applied magnetic field. (2) (3) (4)

Another important property is that the presence of the magnetic field breaks the inversion time T operator. For instance, the presence doesn't allow Kramer's degenerate pairs. And in the same form the Meissner effect of the superconductivity is also related with the quantization of the magnetic flux in the second type of superconductors. (5) (6)

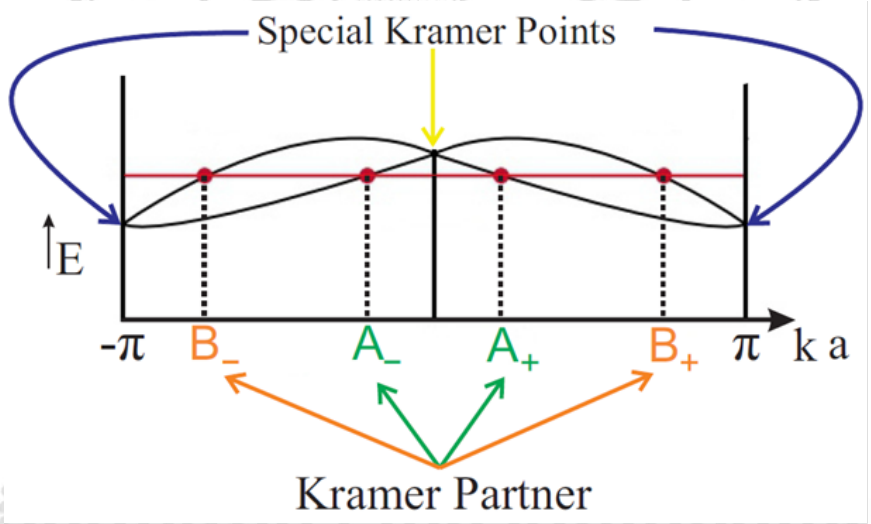

Figure 3.1. Part of the band diagram for spin -1/2 particle with time-reversal symmetry is shown. The points on the **k·a** axis are color-coded to show the Kramer partners. Note that for a fixed energy — horizontal 'red' line — there are four energy eigenstes, and among the four states, A_+ is time-reversal partner of A_-, with equal but opposite **k·a**, likewise for B_+ and B_-. The Special Kramer's Points are those who are their own time-reversal symmetric partner, and this leads to the degeneracy AT those **k** points. (6)

Kramer's theorem (7) is important since it can give us a lot information about a system having two pieces of information, namely 1. the system has total half-integer spin, 2. the time-reversal symmetry is preserved. On top of that, one can predict how the system will respond to a given perturbation, without doing any explicit calculation. Usual

application of Kramer's' degeneracy is for Anderson's theorem for dirty superconductors. (8) Figure 3.1. is graphical representation of Kremer's partner.

This will be important for further explanation of magnetic field influence on chemical reactions that involve radical intermediates, plasma ions, aqueous solutions or excited molecules, (9) as represented at Figure 3.2. Important point of Figure 3.2. are ground, singlet and triplet state. The magnetic field will affect the spin evolution between singlet and triplet states. Affecting spin evolution will affect the yield of chemical product and reaction kinetics.

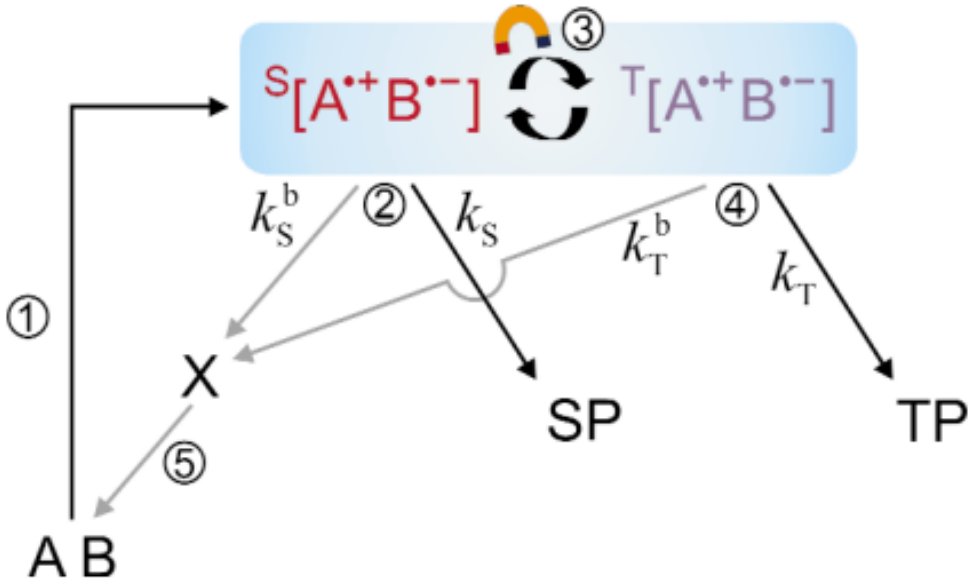

Figure 3.2. Radical pair mechanism, magnetic fields, which act to alter their rate, yield, or product distribution. (10) . ❶ ground state, ❷ singlet product, ❸ singlet and triplet interconversion is driven by magnetic interactions in the radical pair and outside magnetic field, ❹ triplet product, ❺nonselective product that converts back to ground state; copyright UIPAC

Every chemical reaction in which radical or excited atom/molecule is produced, that have unpaired electron and will make a chemical bond and thus pair unpaired electrons. There are two ways of pairing electrons, if paired conventionally the singlet is produced. However, if the spin of one is changed then instead of recombining as a singlet a triplet is formed, again conventionally marked as double electron with same spin (↑↑) and the triplet state may undergo different reactions and not reform the starting compound.

"The triplet state, as the name suggest has three substates which are of equal energy (degenerate) in the absence of a magnetic field. However, two of these states are sensitive

to a magnetic field, one rises in energy, the other falls by an equal amount so that the total energy is constant, (Figure 3.3). The triplet has a higher energy than the singlet, which, as it is spin paired, is insensitive to magnetic fields." (10)

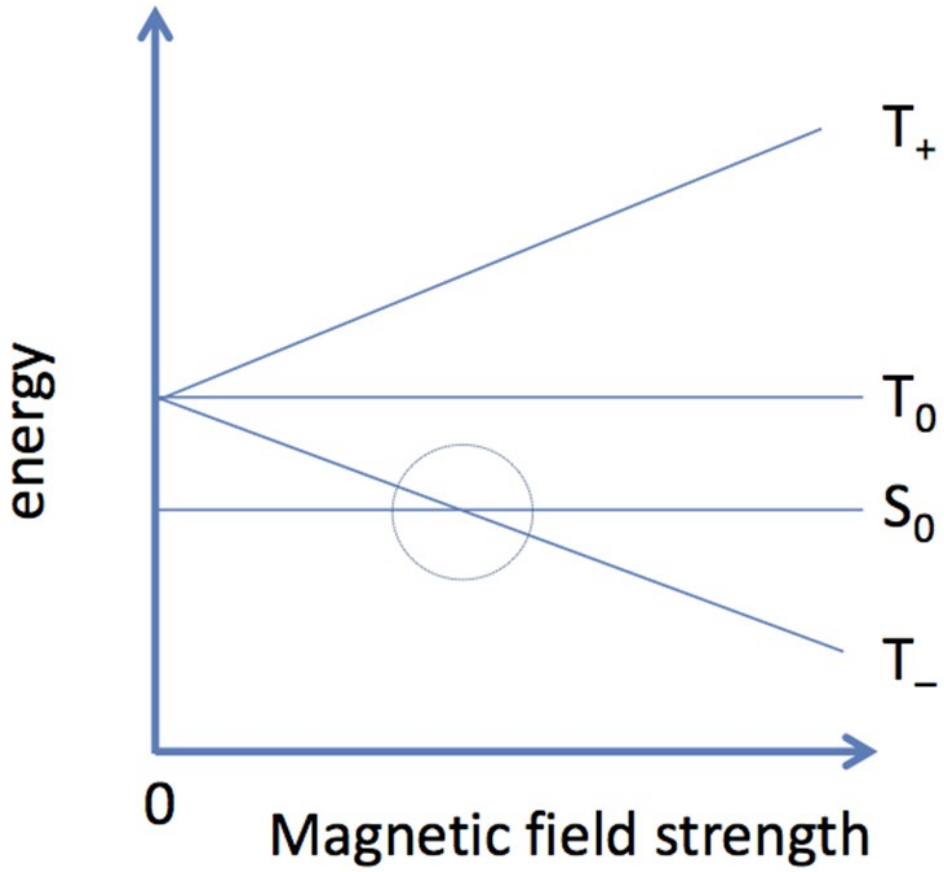

Figure 3.3. three substates of TRIPLET state, circle represent the moment where magnetic field can influence triplet-singlet crossing, (11). Copyright StackExchange

There are many examples of triplet states in magnetic fields as studied by electron paramagnetic resonance (ESR or EPR) experiments.(11) In magnetoreception of birds, (12) protein is called Cry4, and it's part of a class of proteins called cryptochromes - photoreceptors sensitive to blue light, found in both plants and animals. These proteins play a role in regulating circadian rhythms. (13) (14) Additionally, protein crystallization technique was used to produce highly ordered 3D magnetoferritin structures (15), ferritin protein cages as a template-constrained growth.

3.2 Crystallization and Orientation of Liquid Crystals

"Magnetic field effects in chemical systems", (10) "The effects of magnetic fields on chemical reactions" from two different authors (16) (17) and "Chemical Reactions in Applied Magnetic Fields" (18) are review papers important for summarizing current theoretical and experimental scientific progress in this field, however they are not frequent and theory don't necessary follow experimental findings. In recent years, liquid crystals emerged as new trend in novel material discovery, and we will address how they behave inside of magnetic field, however the question of magnetic fields influence on solution crystallization and magnetic memory effect (19) is even today important since there are no scientifically consensus around what is the cause of such an influence on crystallization (20) (21) (22) (23).

Almost half century ago, it was observed influence and effect of magnetic field on molecular alignment, (24) orientation patterns (25) and influence on properties due to preparation in magnetic field (26). In nemetic liquid crystals, magnetic field was used to align single- and multiwalled carbon nanotubes inside liquid crystal block (27), Multiwalled carbon nanotubes can be structurally evolved from fullarens by applying an external magnetic field (28) or even growth (29). Other possibilities of controling liguid crystals are eighter by doping with magnetic nanoparticles (30) and for biocompactible purpose paterning laminar flow with periodic velocity oscillations (31) as presented at *Figure 3.4* of micrographs patterned alignment of the active nematic liquid crystal with a magnetic field. This can be explained by rotating cooperatively in a forces known as a magnetic torque, represented in Figure 4A with red three-pointed star.

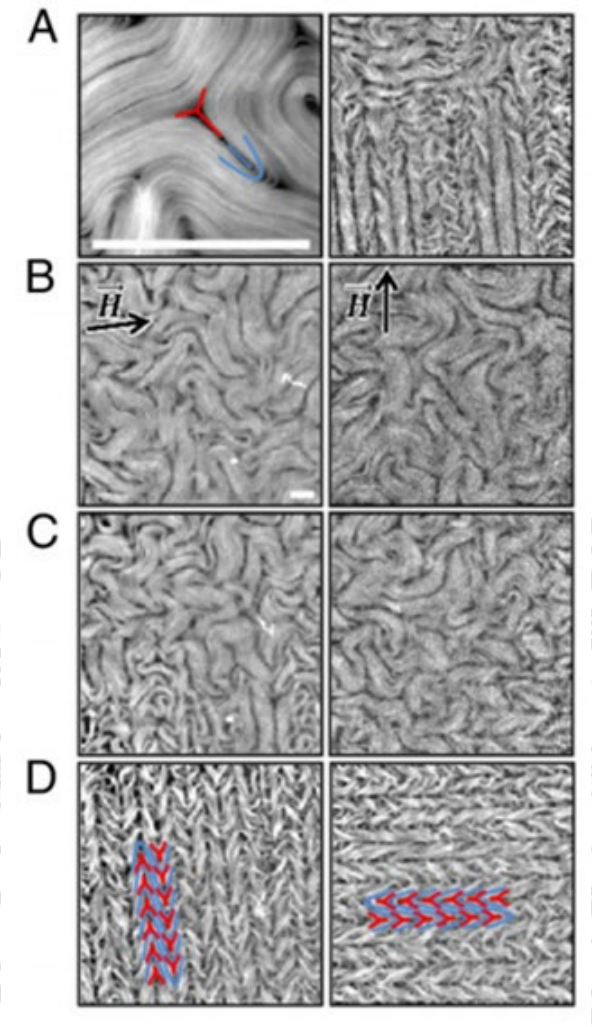

Figure 3.4. Control of liquid crystals structure and movement with unidirectional patterns of laminar flow by applied magnetic field. Magnetic field can easily reestablish initial confuguration by rotating the magnetic field for 90°, (A) Fluorescence micrograph of the active nematic with a pair of complementary +1/2 (blue)and −1/2 (red) defects highlighted. (B) The active fluid is initially in contact with nematic 8CB, which is transited, below T_0 = 33.4 °C, into the lamellar smectic-A phase (C) under a horizontal magnetic field. (D) The active nematic aligns perpendicularly to the field. By temperature cycling above and below initial temperature under vertical magnetic field, the active nematic is now realigned in the orthogonal direction. Copyright PNAS. (31).

There are three typical influences on liquid crystals orientation such as from electric filed, magnetic field and from substrate of the cell. (32) Liquid crystal units or “domains” (33) can align in the same direction and rotate together with magnetic field by magnetic torque (34). If magnetic susceptibility is positive units in liquid crystal molecule will align parallel to the field. (32)

Important product of applied magnetic field on magnetic crystal is a phase transition in an undistorted state of liquid crystal called Fréedericksz transition (35-38), it found first application in simplest liquid crystal display of LCD watch or calculator. Additionally, use of magnetic field during processing of liquid crystals can freely control orientation and whole process is simpler with just a magnetic field instead of using various chemical routes or capping agents. Rokhlenko *et al.* (39) have shown that they can orient sheet-like domains using a magnetic field, due to magnetic anisotropy present in liquid crystal polymer melt. Large magnetic anisotropy was explained by presence of ring structures at each monomer. Each ring has mobile electrons and thus magnetic field can generate field along ring axes, this current flowing on the ring axes will align with external magnetic field. (40)

A. M. Parshin *et al.* (41) studied the structural transformations in the polymer-disperse liquid crystals films formed in 0.4 T magnetic field. They explained influence of magnetic field on structural orientation of liquid crystal as the deviation of the nematic crystal director from the surface of the gel polymer in a magnetic field. In their opinion, this transition is caused by magnetic field-driven weakening of tangential surface anchoring, depending on which is side of transition is stronger it can either focus orientation in the direction of a polymer droplet axis or along the easy orientation axis imposed by the magnetic field.

Considerably weak external magnetic fields of 1 mT strength was used (42) to rapidly and reversibly manipulate ferromagnetic nanorod orientation, that are used as building blocks to construct liquid crystals with specific optical properties. Using alternating magnetic field, liquid crystal exhibited optical switching frequency above 100 Hz. By changing orientation of nanoroads, transmittance intensity can be tuned. In conclusion, two most important processes for structural alignment in magnetic field that give liquid crystal specific properties, from mechanical to optical is magnetically derived torque. R. M. Erb et al. (43), shown at Figure 3.5. determinate three types of Magnetic torque: 1) ferromagnetic torque, 2) paramagnetic torque, and 3) magnetic body-force

torque. For the liquid crystal application first two are important since they are internal and give the energy for movement as shown in Figure 3.4.

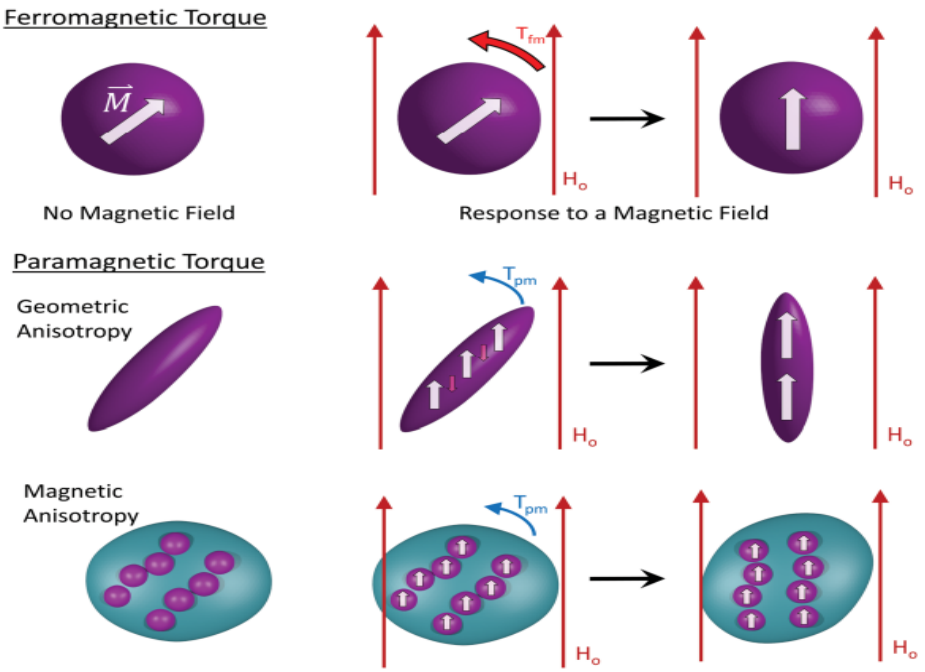

Figure 3.5. Ferromagnetic Torque and Paramagnetic Torques are derived from an internal magnetic restoring torque working to rotate the material to an orientation of lower energy. As claimed by R.M. Erb *et al*. If a paramagnetic particle has geometric anisotropy, the energetics of particle alignment relates to minimizing the internal frustration of a magnetized body. The torque on spherical paramagnetic particles also exhibit some magnetic anisotropy and can be modelled by obtaining the demagnetizing coefficients from experiment, simulation, or a theoretical solving of the magnetic energy of the system at each angle. Copyright: Willey HCM Modified from ref (43).

Regarding magnetic Fréedericksz transition (44), it will depend on the anisotropy of diamagnetic susceptibility of liquid crystal and on the initial mutual orientation of the nematic director and the magnetic moment of domains or molecules inside of liquid crystals. Magnetic Fréedericksz transition is decreased when diamagnetic susceptibility is higher than zero and there is parallel orientation between orientation of liquid crystal and the magnetic moment of "domain". (45) In case of perpendicular relationship between orientation of liquid crystal director and magnetic moment of molecules inside of it and magnetic susceptibility of liquid crystal is more than zero, Fréedericksz transition increases (46) or as well if susceptibility is less than zero but relationship between orientation of director and domain are parallel. However, important exemption is

ferronematic liquid crystals that can be induced by low magnetic fields (less than 0.1T), way below the magnetic Fréedericksz transition threshold. (47)

3.3 **Crystallization of Proteins and Salts**

Mikelson and Karklin, (48) solidified metal alloys melts in magnetic field from 0.5T to 1.5T and they found that primary nuclei of the alloy crystalized is oriented with their longer axes along the lines of force of the magnetic field. They explain crystal orientation effect by magnetic field depending on magnetic properties of crystal nucleus and those of melts. Homogeneity of magnetic field also in their opinion played important role in crystal orientation. Next emphasis of their work is on electron flow generation if the melt which crystalize is conductive when cooling down heterogeneity by phase transition will arise. The last emphasis was influence of applied magnetic field on thermal convection which will define end crystal by influencing viscosity of the melt.

In K. Watanabe *et al*., book (49) the use of magnetic field applied for crystal growth process was for damping convection in semiconductor melts. They also review crystallization of organic molecules and proteins, in ambient condition, this method is beneficial due to possibility of protein denaturation at higher temperature (40°C), therefor they examined crystallization of proteins in 0T, 5T and 11 T applied field, in lower temperature settings. Magnetic field influenced the nucleation process, the ratio of the growth rates of the crystal faces. It was noticed that those tendencies in magnetic field are enhanced by increasing protein concentration. Also, by increasing magnetic field, number of crystals were decreased. According to them, crystallization of protein occurred while they were sedimenting from solution. They conclude that number of crystals oriented with magnetic field, can be increased by using higher concentration of protein and taller cells (crystals grown from taller cells). It was found that a magnetic field decreased the growth rate of the crystals in an electrolyte solution. Crystal quality of proteins is affected by convection and diffusion (mass transport), Da-Chuan Yin (50) in his review determinates several ways on how to control mass transport of proteins crystalization:

- temperature gradient,
- microgravity environment,
- design of the containers,
- ceiling configuration crystallization,

- strong magnetic field,

In non-conductive solution such as protein or other macromolecules, the effect on the convection have the magnetization force, which according Da-Chuan Yin if strong enough (to counteract the gravitational force) can produce condition in solution same as those in microgravity. The damping effect of the Lorentz force on the convection in protein solution is weak. May

Regarding inorganic molecules, there are two direction examining effect of magnetic field on crystallization, one in thermal processing/analysis (51) and other in solution chemistry (52) (sedimentation experiments). In first case, the high magnetic field (up to 20T) was introduced in high temperature environments in order to control material functionality. We can observe two phenomena regarding this case:

A) effect on phase transitions and B) an increase in coercivity of permanent magnets. Iron phase in multicomponent crystalline alloys will increase in the nucleation rate Fe by annealing in magnetic fields, (53) also using spark discharge inside of pure nitrogen atmosphere will obtain different products of nitride (54) or with field above 0.4 T pure zerovalent metals (55).

Regarding solution chemistry, precipitation of 90% of $CaCO_3$ in 1.2 T external magnetic field resulted in sedimentation of aragonite/vaterite crystals. externally applied magnetic field is lowering the zeta potential of $CaCO_3$. (56) Aragonite is formed at high temperature and pressure from melts. Therefore, the formation of calcite is energetically in favour than the one of aragonite. However, why in applied external field, aragonite is formed over calcite? Theoretically this can happen only if magnetic field is 45T, but still researchers achieve it under application of 0.4T high gain of aragonite concentration is achieved. (80%) (57)

Chandrasekhar (52) used 5.5 T field on magnetic on sodium hexafluorosilicate to improve the crystallinity. They explain effect referring to Mitrovic (58,59,60) observation, that Lorentz force influence on ion movement in solution as they pass through magnetic field and slowing down the growth disrupting the regularity of the lattice.

According to Prof. Daniel Baldomir (6), inorganic salts as in example of Calcium Carbonate aka scale formation compound ($CaCO_3$), have no magnetic structure and are diamagnets with negative susceptibility. There are two possible crystalline symmetries,

orthorhombic crystal structure of Aragonite and rhombohedral of Calcite. Solubility in water will decrease with increase in temperature. In Prof. Daniel Baldomir opinion, the main reason why is there modification of the local ionic concentration due ion motion via Lorentz force (qv x **B**). By analogy with the Hall effect (3), assuming velocity (**v**) as 1 meter per second, and magnetic field force 0.1 T, the nonelectrostatic field of 0.1 V/m is associated with surface charge density of 10~11 C/m^2, which can increase ionization and radical formation a lot, enabling singlet-triplet formations.

Prof. Baldomir continues, magnetic field also acts on the charges besides the spins and this can allow a certain substance to have “magnetic” properties, this is not simple for $CaCO_3$ and very difficult to interpret as “magnetic” ions. The usual form for obtaining magnetic order is to need at least some elements with d-electrons when the spins are going to be considered as the fundamental ingredient. Therefore, this compound can be seen as having "magnetic" order with additional needs consider a lot more subtleties, explained further by J.M.D. Coey *et al.* (61) as following three processes that might influence nucleation mechanism for crystallization:

- Contamination with $3d^5$ (S=5/2) ions;
- Hard water and substrate of steel pipe as nucleation activator;
- Local ionic charge and surface charge density;

Mitrovic (59) who conducted synthesis of manganese chloride and Rochelle salt in presence of magnetic field and Ohagaki (62) *et al.* who investigated barium chloride and produced crystals under magnetic field, at ambient and temperature of maximum saturation of solution (50ºC), by them every molecule or ion is regarded as diamagnet and orientation is results of movement and alignment of those diamagnets.

H.E. Lundager Madsen (63), precipitated at 0,27T (25ºC) and found an effect of the magnetic field on carbonates and phosphates with diamagnetic metal ions. In 2008, Tai *et al*, (56) would induce crystallization of $CaCO_3$ in pipes using 0.0074 T magnetic force. They confirmed that aragonite crystals are formed, and calcite growth is inhibited in magnetic field. Permanent magnets outside of steel pipes were 0.1T strong, generating the field inside of pipes, due to Teflon coating, of a 74 gauss. This utilization of weak magnetic force or field is currently finding applications in environmental technology as enhancing absorption and removal of heavy metals and other pollutants (64-68)

By now, we can observe two directions in research of magnetic field application for chemical reaction. One group that use field above 5T for crystallization of alloy melts (69-73) and groups addressing electrolyte crystallization in magnetic field. (74,75)

3.4 Crystallization of metal melts inside of magnetic field

J.M.D. Coey and H.E.L. Madsen, assumed role of water and prenucleation clusters, referred as DOLLOPs. Proton dimers will mix single-triplet change in ionic bond of salts that crystalized under magnetic fields. Why these authors are so vividly focused on water molecules and protons, it appears to be related to historical context. Namely, at that time, there was controversial trend of magnetic treatment water. (76) Researchers never explored possibility that water is just a medium for magnetic field, magnetic field influence on ions outside of solutions. Magnetic spattering was used to increase the density of argon ion plasma, in most of cases chemical reactions such as oxidation and nitridification were not desirable, so effect on chemical reaction of magnetron was suppress, even though this technique is famous and in trend at the same time as crystallization of solutions in presence of magnetic field.(77) This is perfectly understandable due to lack of interdisciplinarity at that time and different purpose of both methods.

Sparking process and arc-discharge are perfect combination for establishing conditions of ionization without solvents and obtaining experimental condition in which chemical reaction can be influenced by magnetic field. (28,54,78)

Two approaches can be deducted for explaining crystallization in magnetic fields, first is represented by the effect of ground vs exited state of metals and second as valence electrons ordering. These deducted from formation of metal ions in liquids and alloys, (79) and size of atom/ion/molecule effect. (80)

Hartmann number is without dimension unit that describes a measure of the relative importance of Laurenz forces arising from external magnetic field and viscous forces in Hartmann flow, and clarifies the velocity profile for such flow. Hartmann flow is the flow of a conductive melt fluid between parallel planes with a magnetic field normal to them. Hartmann Number will specify the relation between the magnetic viscosity and the ordinary viscosity and if Lorentz force have role in crystallization. It is calculated as

$Ha = BL\sqrt{\frac{\sigma}{\mu}}$; B is the magnetic field intensity applied on the plasma or melt, L is the distinctive length scale of flow, σ is the electrical conductivity of metal, μ is the dynamic viscosity which is proportional to a product of kinematic viscosity and density of the fluid. This dissertation is first to report ambient temperature (low-temperature crystallization. First point is to prove influence of Lorentz force on crystallization. In sparking process, it was applied weak magnetic field from 0.1 Tesla to 0.4 Tesla, substitution in Hartmann number formula on sparking gap of 2 millimetres the value is below 30 and for Lorenz force to have any significant impact Hartmann number need to be above 100. Calculated values represented in Table 5.

Table 5. Hartmann number calculation for sparked iron wire

Units	Values	References
B- magnetic field	0.4 T	Tesla, 4000 gausses
L- spark length	2 mm	$2*10^{-3}$ meter
σ - electrical conductivity	1.3 μS/m	(81)
μ- dynamic viscosity	35055.2 η	Density of iron 7034.96 kg m^{-3}, viscosity of molten iron 4.983 η/mPa s (82)
Hartmann number	29	$Ha = BL\sqrt{\frac{\sigma}{\mu}}$

3.5 Results and discussion

"Longevity prolongation" as it is observed with over period of time, is described as a chemical state in which Iron is resistant to oxidation at ambient conditions. In environmental science, three processes are identified for preventing total oxidation of nZVI; aging, vacuum annealing, and coating. (83) However, magnetic force for longevity prolongation has not been used before, and it has the potential for being of great importance in the future for all ferromagnetic materials. If we compare amorphous form (either organic or inorganic) with crystallized form, we can clearly observe that amorphous substances oxidize and dissolve faster and have a better bioavailability in therapeutic sense. Li et al (84) claims that high crystallized bimetallic nanoparticles provide ease of storage and transportation and describes how

highly crystallized PtCu helps to achieve enhanced stability and recoverable surface. Crystallization of nanoparticles is a complicated process, especially Single Crystalline Thin Films. In our case, we overcome this by sparking inside of a magnetic field-for Iron 0.4T to achieve single pick (Figure 3.6a). How did we experimentally prove that longevity of nZVI is prolonged? By XPS (Table 6.), XRD analysis measured at different time intervals from synthesis (up to 90 days of exposure to air until right after synthesis measurement). Longevity, based on our experiment with nZVI, implies high crystallinity of Iron nanoparticles, which was never described or reported before and is useful for storage (which we proved in the experiment) and potentially other purposes, such as reactivity and longevity in solutions, which was not experimentally proved in this manuscript, since our scope was to demonstrate how to increase crystallinity of iron nanoparticles.

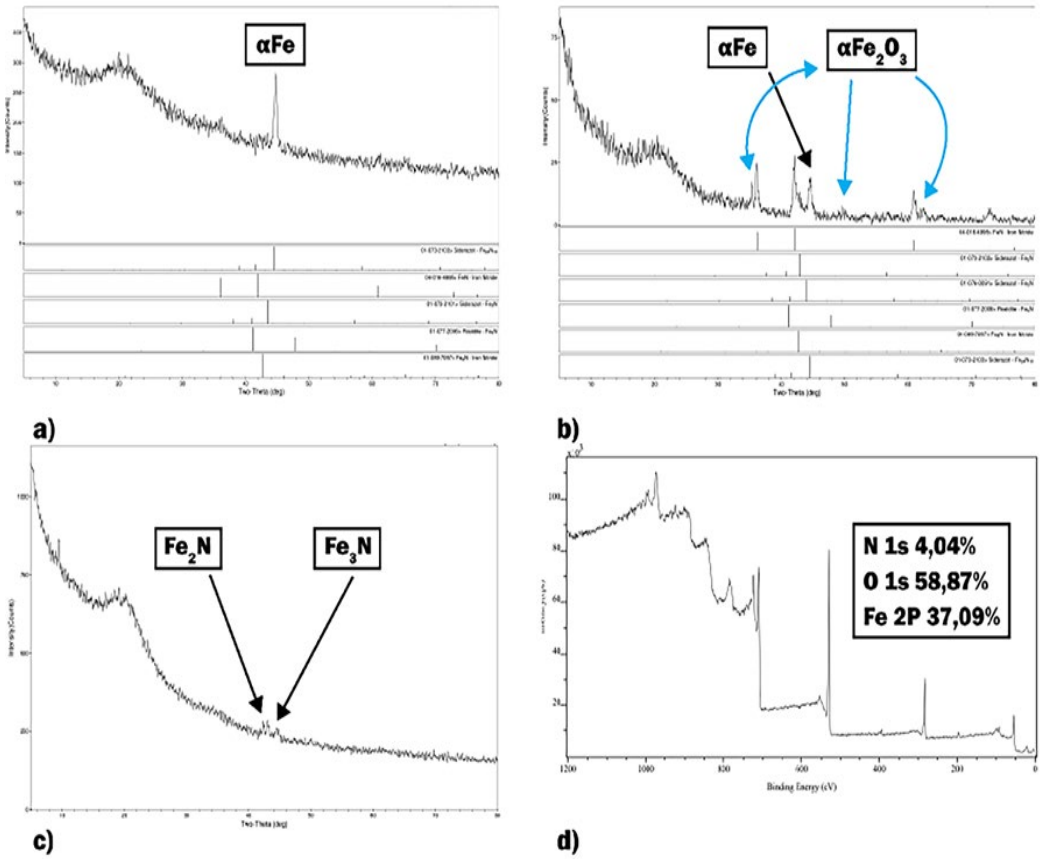

Figure 3.6 Characterization of longevity and crystallinity of sparked iron a) XRD results of iron thin film prepared inside of magnetic field, 0.4 Tesla; b) XRD results of iron thin film prepared at 0.2 Tesla; c) Iron thin film sparked without magnetic field; d) XPS results of sample prepared in 0.2 Tesla confirming existence of nitrogen phase and therefore nitride. (54).

Table 6. Comparative representation of nitrogen peaks in XPS spectra prepared under different conditions: (a) no data – no observed peak at N 1s; (b) no substrate – the sample did not survive after exposure to the air; (c) (—) not done

N 1s (T)	Fresh sample	Aged 90 days	Aged 120 days
0	No data	398 44	No substrate
0.1	400 027	—	—
0.2	396 300	396 737	396 218
0.3	—	—	399 931
0.4	No data	No data	No data

Reference 54.

3.6 Hypothesis that higher crystalline phase implies longevity

What is the purpose of vacuum annealing? Crystallinity of the system depends on the cooling rate of the system from the heat treatment temperature to room temperature. If the system is cooled slowly and in a controlled manner, one can observe an increase in crystallinity of the system. Other purposes are to protect nanomaterials from residual stress, oxidation, and enable equal morphology. Vacuum annealing is one of the methods for longevity prolongation, however, the process is expensive and energy consuming, which is problematic for environmental applications and in general. We experimentally proved higher crystallinity by sparking iron wire in 0.4 T under inert atmosphere and confirmed the results via TEM, SAED, GIXRD, and XPS analysis of fresh samples, as well as samples aged for 90 and 120 days. We also performed several subsequent analyses of thin films prepared in different magnetic fields (0T, 0.2T and 0.4T) and exposed to ambient air for different lengths of time (None, 90 days and 120 days). Samples were first checked with EDX and SAED. The results of EDX-SEM showed no sign of oxygen or core shell structure, further examination with TEM-SAED showed a match with d-spacing of iron and iron-nitride phases in JCPDF database. Based on these results, we further investigated these films with GIXRD and XPS techniques under different conditions. Parameters used were sparking of iron wire inside different magnetic fields, rotation of substrate, and subsequent exposure to air. Constant high flow rate of nitrogen or other inert gas was used in study. With the rate of 600 L per second, higher pressure inside sparking chamber than outside was maintained, preventing any oxygen infiltration. What was done to prevent oxidation during synthesis will further be described in section

about replicability and quality control of experiment. The sample exposed to air was also checked for crystalline phase changes and bonding energy of substrates. The results of these characterizations should prove sufficient to support the claim of longevity, since, as stated previously, what is meant by longevity is a low oxidation rate of nZVI.

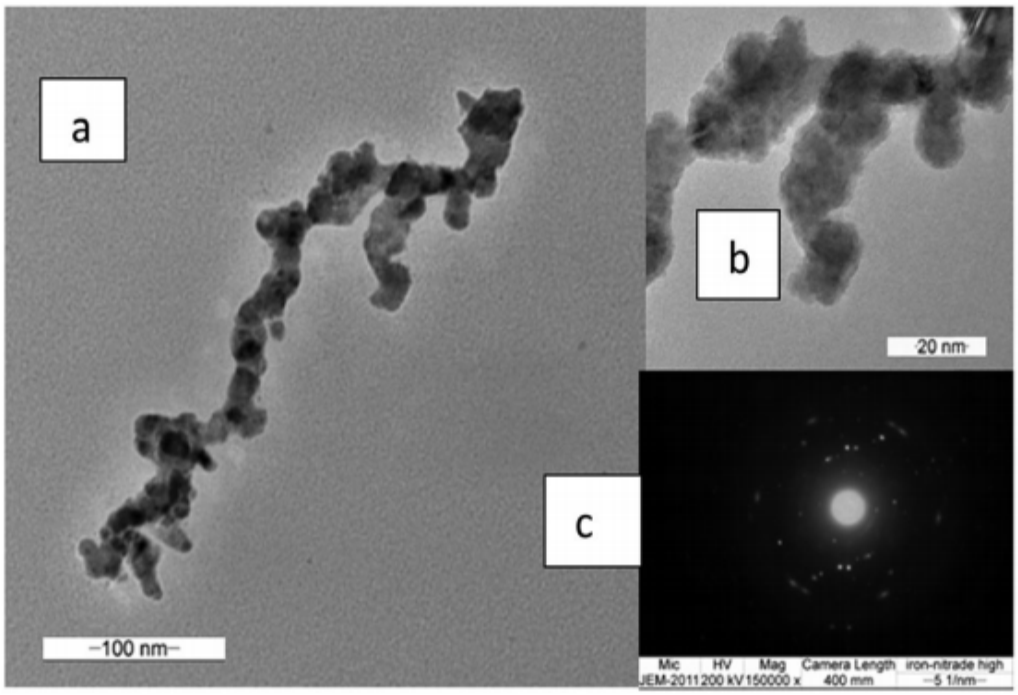

Figure 3.7 TEM image of Iron wire sparked inside of 0.2 T at nitrogen flow. (54)

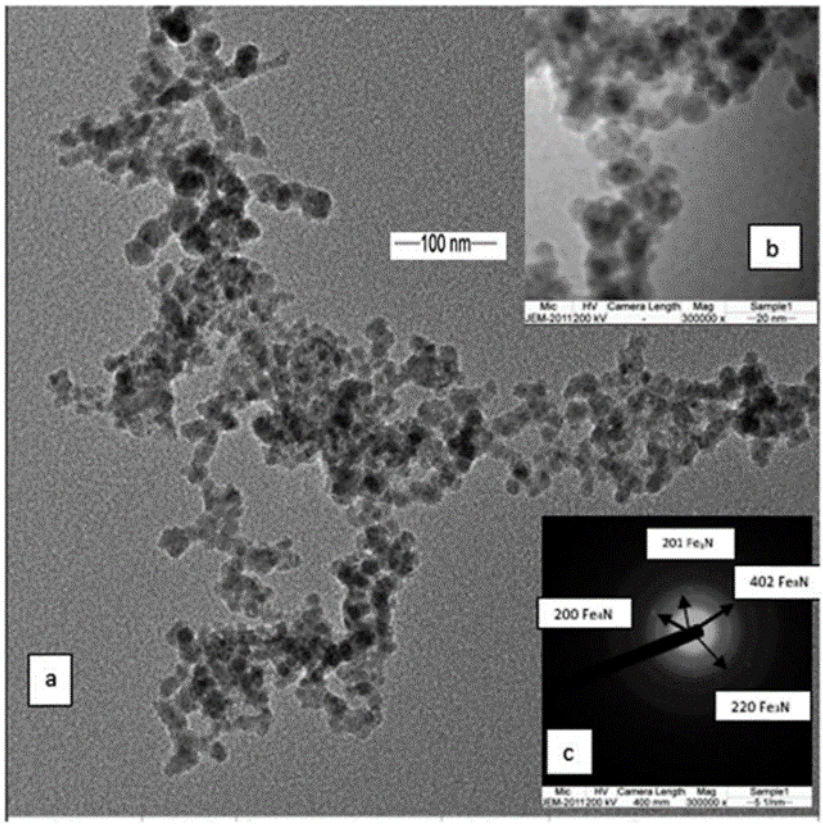

Figure 3.8 TEM image of iron nanoparticles sparked inside of 0.4 Tesla under nitrogen gas flow. (54)

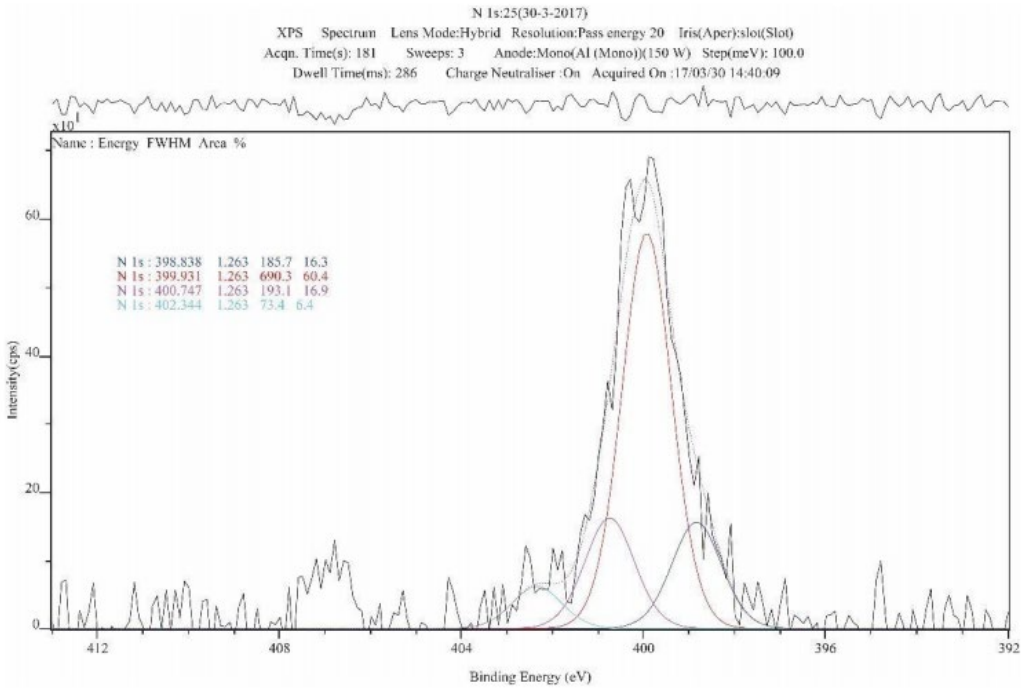

Figure 3.9 XPS spectrum of Nitrogen N 1s binding energy of iron thin film sparked inside of 0.2 Tesla under Nitrogen flow conditions. (54)

3.7 Chemical reactions of iron and nitrogen. Environmental technology

According to EU guidelines for "eco-friendly" technology and EU investments to project "BOUNAPART-E", EU is investing in scaling up of the sparking discharge process. This process doesn't use precursors, can utilize recycled materials, broad range of elements, and has a minimal waste production compared to other methods. It also consumes less energy than arc-discharge process. Spark discharge is also known as Sparking process, Spark ablation, Spark melt, and Electric discharge machining. On the Current Density–Voltage Curve (Figure 3.10), spark regime is at breakdown voltage point that is between the corona discharge in Townsend regime of dark discharge, and the glow discharge, as explained in Electric glow discharge (85).

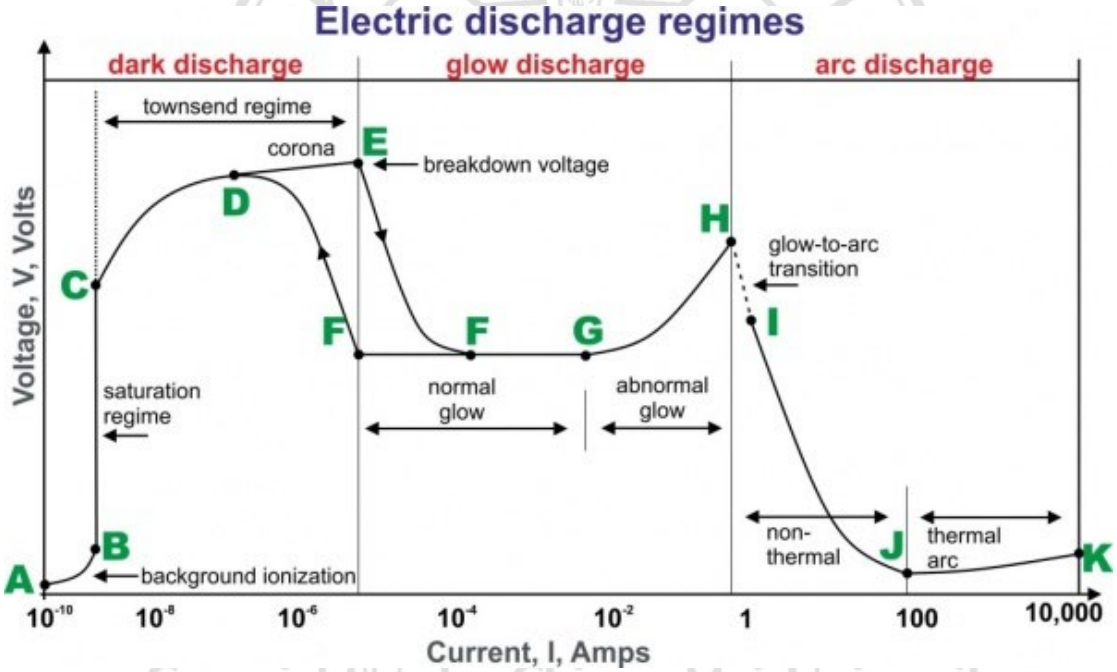

Figure 3.10 Voltage-current characteristic of discharge, sparking belongs to point E. (85)

In a chemical sense, there is a vapor of metal and a plasma channel in between of metal wires. For this thesis that will mean that is obtained Iron plasma (ionized iron) and vaporized iron, which are susceptible to a magnetic field. Therefore, the reaction between ionized or vaporized iron and nitrogen can be affected by the magnetic field as is the case for chemical reactions that involve radical intermediates. The magnetic field alters their rate, yield, or product distribution. (10) Nitrogen gas is not reactive by itself and the process of breaking the triple bond between nitrogen atoms requires considerable amount

of energy, however, our experimental setup succeeded to excite nitrogen gas molecule with sparking discharge. The mechanism of excitation is already used in the nitrogen laser, where electric current is discharged trough nitrogen gas. In our experiment, the sparking head is modified for holding adjustable iron wires with a space gap between wires starting at 2 mm and widening to 6 mm due to the consuming of wire over the time of sparking. Knowing that when the distance between wires' tips is 10 mm, the air is dry, the temperature is between 100 and 300 K, the breakdown voltage of nitrogen is 30kV (86) and our electronic setup resembles the one used in the nitrogen laser (The electronics of the nitrogen laser are a circuit composed of a spark gap, a capacitor, and the discharge through the nitrogen. First the spark gap and the capacitor are charged. The spark gap then discharges itself and voltage is applied to the nitrogen.) with a spark gap of 2mm and iron wire 1 mm thick. The processes occurring in the nitrogen laser are UV generation, ionization, and electron capture. All reactions with radicals (plasma, ions, excited gasses) are influenced by magnetic fields since they have unpaired electrons. Pairs of radicals are formed when these radicals have a broken chemical bond and are in close proximity. These pairs are called geminats. These two excited or/and ionized molecules can then form a new chemical bond. In this case the spins are paired and produce a singlet. However, if the spin of one is changed then instead of recombining as a singlet, a triplet is formed. The triplet state may undergo different reactions and not reform the starting compound. The triplet state has three sub-states which are of equal energy (degenerate), however, they have a higher energy than the singlet, which, as it is spin paired, is insensitive to magnetic fields. Normally, the difference in energy between a singlet and a triplet is large, compared to thermal energy, which makes the singlet-triplet crossing very slow and is unimportant in the absence of a magnetic field. (The energy gap at zero magnetic field is 2*J* where J is the exchange energy); One of the triplet sub-states remains of a constant energy, while the energy of the other two changes. These sub-states are the ones that are influenced by a magnetic field. Of them, the energy level of one sub-state rises and of the other falls by an equal amount. The sub-state with the falling amount of energy can reach the energy level of a singlet and it is at this point that a magnetic field facilitates rapid crossing from singlets to triplets and thus to the possibility of a different chemistry of radicals. As the crossing is quite narrow, in terms of the range of magnetic field strength, only if the magnetic field is of just the right value will singlet-triplet

crossing occur. The field strength needed to cause singlet-triplet crossing is typically of the order of a few hundred Gauss (10^4 gauss = 1 Tesla). Magnetic field also influences triplet-triplet annihilation and electron transfer. The energy levels of a triplet molecule are split when a magnetic field is applied.

3.8 Effect of the magnetic field on the reaction between Iron and Nitrogen and effect on crystallization

The intensity of the peak obtained by GIXRD significantly improved from amorphous form (weak peak on 0 Tesla) through polycrystalline form (0.2T; mixed phases of Iron, Iron Nitride and artefacts of Iron oxide) to the sample sparked at 0.4 T which exhibited a strong peak of Iron. COD number for Iron detected Fe (COD:04-006-4004) and FeN (04-016-4995) for a sample prepared at 0.2T, and at 0.4T, Fe (00-006-0696). For a sample prepared at 0T Fe (COD:04-006-2179), COD was determined by using HighScore Plus software of PANalytical as shown on Figure 3.11. Nitride peak on XRD of the sample prepared at 0.2T was consistent even after 120 days of ageing at ambient conditions. There are two possible routes for reaction to occur. First by mixing metal vapor, which traps nitrogen, with nitrogen gas, thus explaining 1:1 ratio. Second by applying a magnetic field on iron plasma and ionized nitrogen, which at 0.2T results in different reaction kinetics and products, compared to other magnetic field, which was also confirmed by XPS, comparative analysis of Nitrogen binding energy on thin films sparked inside of 0T, 0.1T, 0.2T, 0.3T, 0.4T, showing binding energy of N 1s at 396.3, consistent with other XPS results of FeN obtained by dc magnetron sputtering (87) (88).

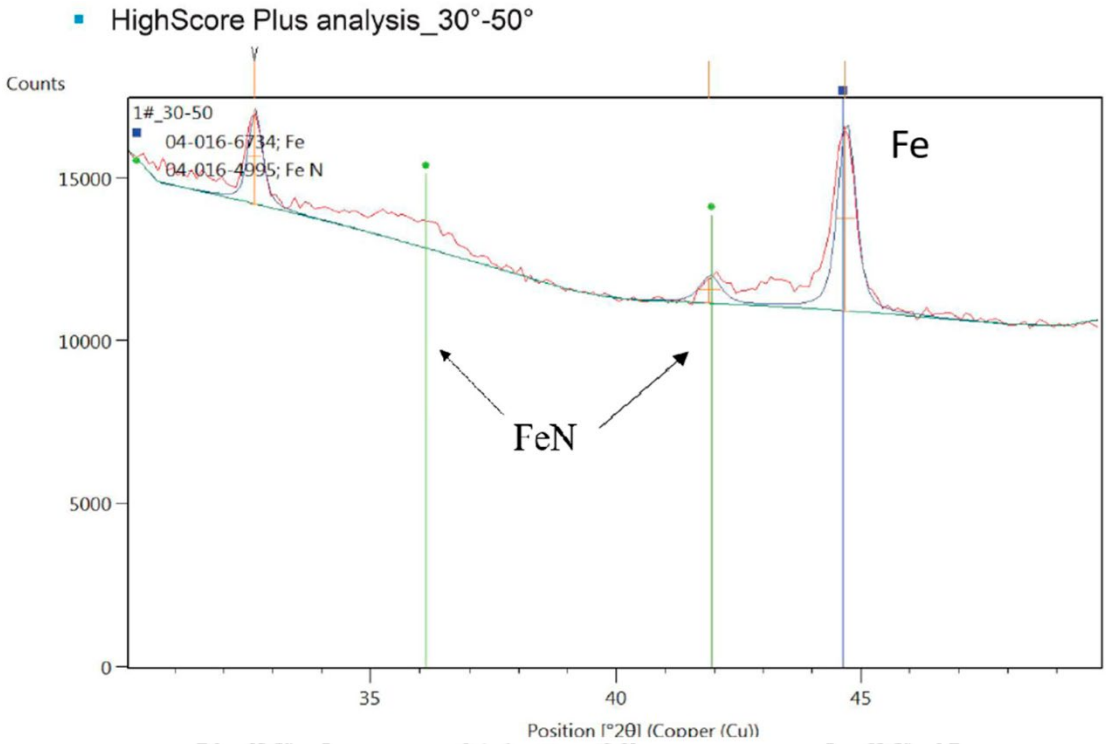

Figure 3.11 GIXRD HighScopre Plus PanAnalytical analysis of iron nitride thin films, aged on atmospheric condition for one year. Blue square represents Iron phase (04-016-6734) and green circle Iron-nitride phase (04-016-4995). (55).

3.9 Replicability and quality control of experiment

Particle morphology changed with the use of argon flow versus nitrogen flow in the chamber. This was further investigated using EDX and SAED studies, which lead me to discover polycrystalline structure that contains nitride d spacing and caused me to explore this occurrence, using XRD investigation. Unfortunately, since the thin film was amorphous or low crystalline, it was unable to gather more information. RAMAN (Figure 3.12) was also unable to confirm the nitride phase, since the laser available was suitable for oxide only. A recommended annealing the sample, however, this is a time and power consuming process which is not appropriate for environmental and scaling-up reasons. Our lab has neodymium-based magnets suitable for collecting nanoparticles in air. Collecting in liquid was also an option but loses were the same as with a simple solid substrate. (See DLS results represented at Figure 3.13) A magnet proved the correct choice since when sparking in inert atmosphere, zerovalent iron nanoparticles are formed, which are of ferromagnetic nature. Pisith et al, used this method to synthesize zerovalent metal nanoparticles of nickel, cobalt and copper in inert atmosphere with the purpose of

growing carbon nano-tubes. Obtaining metal nano-particles is already reported by Schmidt-Otto research group. They all had problem with achieving crystallization. All samples were annealed. Additionally, losses during production were substantial, as is the case with all aerosols synthetized in large and ambient conditions. Nanoparticle dust/aerosol generation by sparking head significantly decreased when a magnet was introduced. This was confirmed by ICP-MS, by swapping chambers and comparing amounts of iron on substrate. (Table 7) Peaks that appeared on XRD results were of higher intensity. These preliminary findings of increased crystallinity and decreased nanoparticle loss were crucial for establishing a viable experimental setup to determinate if Nitride phases were formed and see the effect of magnetic field presence on XRD peak intensity. Experimental setup and quality control:

1.) Assuring nitrogen quality and prevention of oxygen infiltration in the chamber. This was achieved by using ultrahigh purity of nitrogen gas and maintaining slightly higher pressure in the chamber than outside of the chamber. Iron wires had no visible signs of corrosion and required no polishing or do any pre-treatment.

2.) Second issue is with sparking onto TEM substrate, which can lead to annealing of nanoparticles with copper grid, and oxidation to which samples could be exposed while handling for microscopy and spectroscopy characterization. This was solved with energy-dispersive X-ray spectroscopy and SAED in order to screen for oxygen and measured spacing, which was compared with JCPDS file database of . Additional characterization was done with Raman and XRD.

3.) Third issue is matching of diffraction pattern from FeO wustatie phase with FeN. Both compounds are cubic with almost equal lattice parameters and the same set of the systematic absences, so the positions of the peaks should be approximately equal. However, the structure is completely different: FeN has a sphalerite structure (F-4 3 m) and FeO has a rock-salt structure (Fm-3 m). This was resolved by XPS.

4.) XPS analysis discovered different nitrogen N 1s, binding energy at different magnetic field-0T,0.1T,0.2T,0.3T and lack of nitrogen N1s at 0.4T. For clarity, I will use table representation of binding energy. All XPS graphs are attached as Electronic supporting information in appendix section of thesis. Elementary analysis of thin film by XPS is also represented there, proving the existence of nitrogen content inside of film.

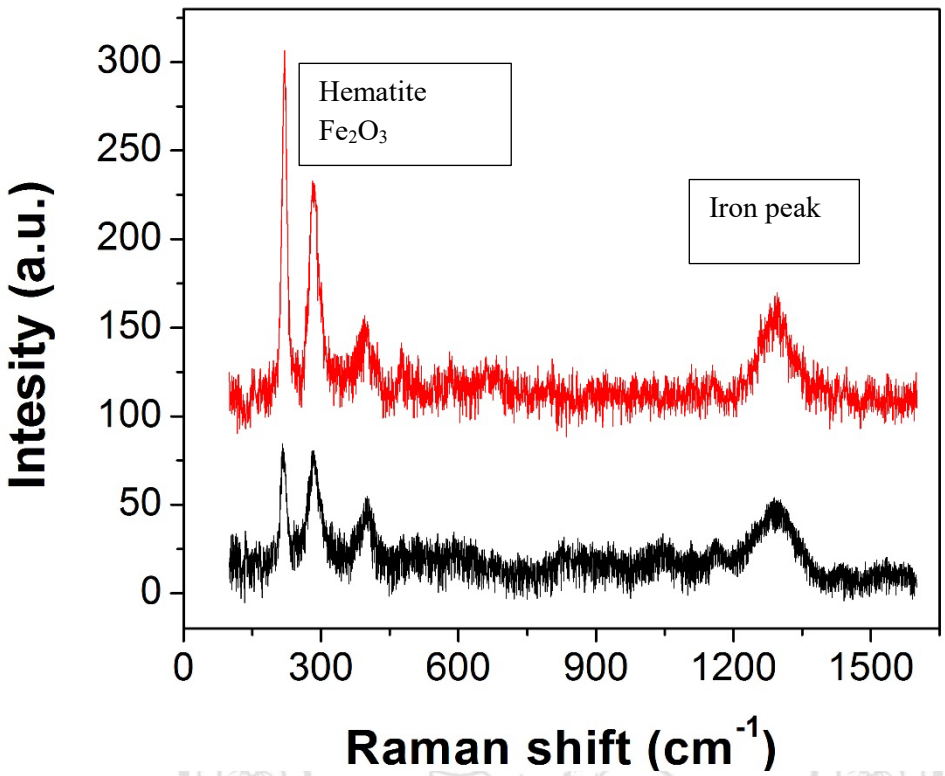

Figure 3.12a Raman spectrum of Iron wire sparked inside of oxygen atmosphere.

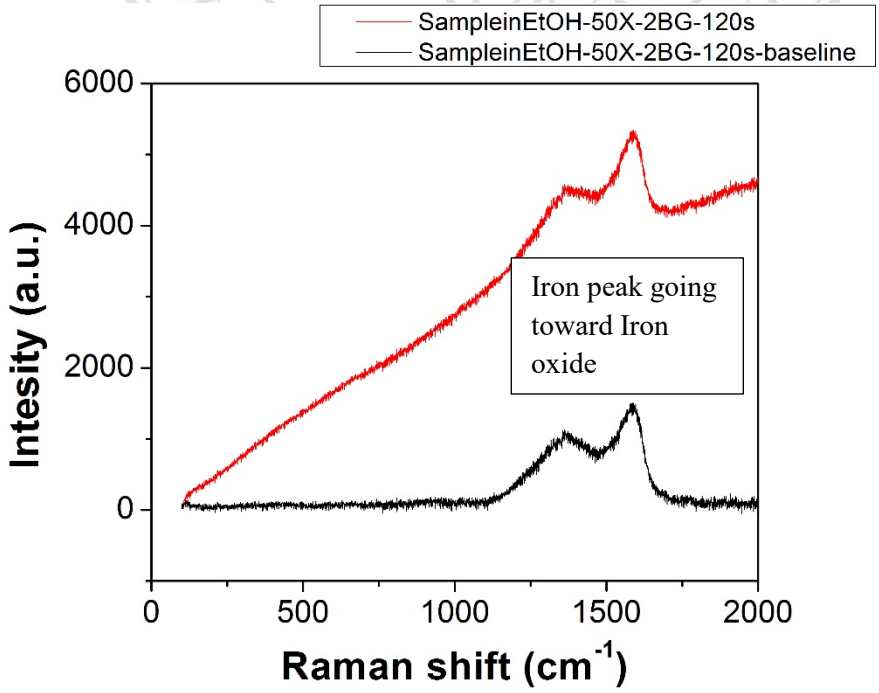

Figure 3.12b Raman spectrum of Iron wire sparked inside of argon atmosphere collected inside of ethanol with magnetic field precipitation.

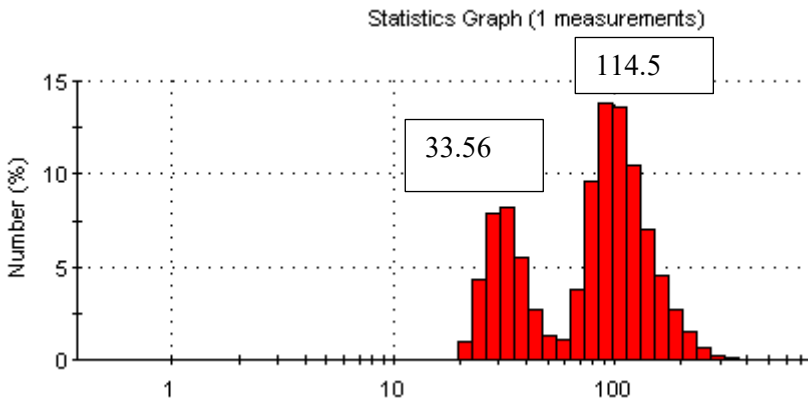

Figure 3.13 Dynamic light scattering of iron wire sparked inside of water. Z-average 144.42 nm. First peak 33.56 nm and Second peak 114.5 nm. Z-average includes precipitated sizes and aggregated sizes from average.

Table 7. Dependence of Iron production by spark discharge on time used for sparking and capacitor size. Measured by ICP. Time versus Capacitor size.

Capacitance	**Sparking time, obtained Iron concentrations in mg/L**					
	5 min	**15 min**	**30 min**	**45 min**	**1 hour**	**2 hours**
10 µF	12	34	69.7	114	290.5	562.7
20 µF	16	42.7	86.4	168	332.6	687
25 µF	18.4	52.8	100.4	182	347	775.3
40 µF	24 1	68.2	124.7	205	492	1025
50 µF	29.6	84.3	137.6	265	567	1331.6
100 µF	31.5	89.6	178.2	302,5	570.2	1401

3.10 High oxygen content in Iron thin films prepared by sparking process

Total mass concentration of oxygen in sparked iron thin film sample according to XPS results that are available in Appendix of the end of this thesis as published in Electronic Supporting Information for New Journal of Chemistry of paper "A Novel strategy for longevity prolongation of iron-based nanoparticles thin film by applied magnetic force" represent of approximately 25%. There is oxygen phase in Raman as depicted at Figure 3.12 or we can see a hematite phase in XRD results of sample prepared in 0.2 T as shown on Figure 3.6b. These oxygen contaminations can be explained as aging or oxidation by exposure to ambient air, oxygen from substrate of silicon oxide that is included in XPS results but as also reactivity of charged and hot iron nanoparticles produced via sparking process and this reacting with surface of silicon oxide. This was especially important while preparing the samples for TEM, and SAED. Because of highly charge particles and high voltage, sparking on copper grid turn to be very challenging and source of many contaminations that were double checked by EDS. However, after several trials and errors SAED results show no oxide phase in freshly prepared samples. XPS results of oxygen peak show peak representing iron oxides 529.9 and rest of peaks were identified as silicon oxide (SiO_2) and organic C-O or C=O contamination.

3.11 References

1. Sasaki Shōsuke. *Theory of the Integer and Fractional Quantum Hall Effects*; Nova Science Publishers Incorporated, **2016**.
2. Eisenstein, J.; Lilly, M.; Cooper, K.; Pfeiffer, L.; West, K. New Physics in High Landau Levels. *Physica E: Low-dimensional Systems and Nanostructures* **2000**, *6*(1-4), 29–35.
3. Tong, D.; Lectures on the quantum Hall effect **2016**. arXiv preprint arXiv:1606.06687.
4. Baldomir, D.; Faílde, D. On Behind the Physics of the Thermoelectricity of Topological Insulators. *Scientific Reports* **2019**, *9*(1).
5. Hirsch, J. E.; Dynamics of the Meissner effect: how superconductors expel magnetic fields respecting Alfven's theorem. Bulletin of the American Physical Society 2018.
6. Interview with Professor Daniel Baldomir, Head of the Technological Research Institute, Department of Applied Physics, University of Santiago de Compostela https://www.researchgate.net/profile/Daniel_Baldomir, retrieved 28th Dec. 2018 from webpage: https://www.researchgate.net/post/Why_magnetic_field_have_influence_on_non-magnetic_materials.
7. Schrieffer, J. R. (2018). Theory of superconductivity. CRC Press.
8. Interview with Mehedi Hasan, Quora user: https://www.quora.com/profile/Mehedi-Hasan-14, https://metalab.ifmo.ru/people/~hasan, from Division of Physics and Applied Physics, Nanyang Technological University, Singapore, retrieved from webpage https://www.quora.com/What-is-the-significance-of-Kramers-degeneracy-theorem.
9. Anderson, P. Theory of Dirty Superconductors. *Journal of Physics and Chemistry of Solids* **1959**, *11*(1-2), 26–30.
10. Rodgers, C. T. Magnetic Field Effects in Chemical Systems. *Pure and Applied Chemistry* **2009**, *81*(1), 19–43.
11. Answer of StackExchage User, “porphyrin”, https://stackexchange.com/users/8473440/porphyrin, answer found on Chemistry StackExchange, retrieved from

https://chemistry.stackexchange.com/questions/24507/can-magnetic-fields-affect-a-chemical-reaction, retrieved on 28th Dec. 2018;

12. Taken from following website, contribution of ref 11 StackExchage User, https://chemistry.stackexchange.com/questions/94578/help-understanding-external-magnetic-field-sensitivity-of-radical-pair-reaction?noredirect=1&lq=1. Accessed on 28th Dec. 2018
13. Solov'Yov, I. A.; Schulten, K. Reaction Kinetics and Mechanism of Magnetic Field Effects in Cryptochrome. *The Journal of Physical Chemistry B* **2012**, *116*(3), 1089–1099.
14. Pinzon-Rodriguez, A.; Bensch, S.; Muheim, R. Expression Patterns of Cryptochrome Genes in Avian Retina Suggest Involvement of Cry4 in Light-Dependent Magnetoreception. *Journal of The Royal Society Interface* **2018**, *15*(140), 20180058.
15. Kasyutich, O.; Sarua, A.; Schwarzache, W. Bioengineered Magnetic Crystals. *Journal of Physics D: Applied Physics* **2010**, *43*(17), 179801–179801.
16. Mclauchlan, K. A. Effects of Magnetic Fields on Chemical Reactions (72 Literaturangaben). *Chemischer Informationsdienst* **1982**, *13*(36).
17. Atkins, P. W. The Effects of Magnetic Fields on Chemical Reactions. *Chemically Induced Magnetic Polarization* **1977**, 383–392.
18. Pankhurst, Q. A.; Parkin, I. P. Chemical Reactions in Applied Magnetic Fields. *Magnetism: Molecules to Materials IV* **2001**. 467–481.
19. Wang, J.; Luo, Z.; Liang, Y.; Li, Z.; Wang, L. Effect of Electromagnetic Fields on Calcium Carbonate Solution Crystallization and Magnetic Memory Effect. *Crystal Research and Technology* **2018**, *53*(6), 1700188.
20. Nakahira, A.; Murase, H.; Yasuda, H. Effect of Application of a High Magnetic Field on the Microstructure of Fe Substituted Layered Double Hydroxide Clay for a Magnetic Application. *Journal of Applied Physics* **2007**, *101*(9).
21. Putro, T.; Endarko. The Influence of Electron Discharge and Magnetic Field on Calcium Carbonate (CaCO3) Precipitation. **2016**. In AIP Conference Proceedings (Vol. 1725, No. 1, p. 020067). AIP Publishing.
22. Chibowski, E.; Szcześ, A. Magnetic Water Treatment–A Review of the Latest Approaches. *Chemosphere* **2018**, *203*, 54–67.

23. Chibowski, E.; Szcześ, A.; Hołysz, L. Influence of Magnetic Field on Evaporation Rate and Surface Tension of Water. *Colloids and Interfaces* **2018**, *2*(4), 68.
24. Carr, E. F. Influence of Electric Fields on the Molecular Alignment in the Liquid Crystalp-(Anisalamino)-Phenyl Acetate. *Molecular Crystals* **1969**, *7*(1),253–268.
25. Leslie, F. M. Distortion of Twisted Orientation Patterns in Liquid Crystals by Magnetic Fields. *Molecular Crystals and Liquid Crystals* **1970**, *12*(1), 57–72.
26. Saupe, A. Recent Results in the Field of Liquid Crystals. *Angewandte Chemie International Edition in English* **1968**, *7*(2), 97–112.
27. Lynch, M. D.; Patrick, D. L. Organizing Carbon Nanotubes with Liquid Crystals. *Nano Letters* **2002**, *2*(11), 1197–1201.
28. Roslan, M.; Rahman, M. A.; Jofri, M.; Chaudary, K.; Mohamad, A.; Ali, J. Fullerene-to-MWCNT Structural Evolution Synthesized by Arc Discharge Plasma. *C* **2018**, *4*(4), 58.
29. Roslan, M.; Chaudhary, K.; Doylend, N.; Agam, A.; Kamarulzaman, R.; Haider, Z.; Mazalan, E.; Ali, J. Growth of Wall-Controlled MWCNTs by Magnetic Field Assisted Arc Discharge Plasma. *Journal of Saudi Chemical Society* **2019**, *23*(2), 171–181.
30. Kopčanský, P.; Tomašovičová, N.; Gdovinová, V.; Timko, M.; Éber, N.; Tóth-Katona, T.; Jadzyn, J.; Honkonen, J.; Chaud, X. How to Enhance Sensitivity of Liquid Crystals to External Magnetic Field? *Acta Physica Polonica A* **2015**, *127*(2), 157–162.
31. Guillamat, P.; Ignés-Mullol, J.; Sagués, F. Control of Active Liquid Crystals with a Magnetic Field. *Proceedings of the National Academy of Sciences* **2016**, *113(20),* 5498-5502.
32. Andrienko, D. Introduction to Liquid Crystals. *Liquid Crystals***2018**, 1–21.
33. Kimura, T. Study on the Effect of Magnetic Fields on Polymeric Materials and Its Application. *Polymer Journal* **2003**, *35*(11), 823–843.
34. Fu, S.; Tsuji, T.; Chono, S. Effect of Magnetic Field on Molecular Orientation of Nematic Liquid Crystalline Polymers under Simple Shear Flow. *Journal of Rheology* **2008**, *52*(2), 451–468.
35. Caussarieu, A.; Petrosyan, A.; Ciliberto, S. Dynamics of a Liquid Crystal Close to the Fréedericksz Transition. *EPL (Europhysics Letters)* **2013**, *104*(2), 26004.

36. Yang, K. H. Freedericksz Transition of Twisted Nematic Cells. *Applied Physics Letters* **1983**, *43*(2), 171–173.
37. Serra, F.; Buscaglia, M.; Bellini, T. The Emergence of Memory in Liquid Crystals. *Materials Today* **2011**, *14*(10), 488–494.
38. Zakhlevnykh, A. Threshold Magnetic Fields and Fréedericksz Transition in a Ferronematic. *Journal of Magnetism and Magnetic Materials* **2004**, *269*(2), 238–244.
39. Rokhlenko, Y.; Gopinadhan, M.; Osuji, C. O.; Zhang, K.; O'Hern, C. S.; Larson, S. R.; Gopalan, P.; Majewski, P. W.; Yager, K. G. Magnetic Alignment of Block Copolymer Microdomains by Intrinsic Chain Anisotropy. *Physical Review Letters* **2015**, *115*(25).
40. Kornei, K. Magnetic Field Aligns Polymer Structures. *Physics* **2015**, *8*.
41. Parshin, A. M.; Nazarov, V. G.; Zyryanov, V. Y.; Shabanov, V. F. Magnetic-Field-Induced Structural Transition in Polymer-Dispersed Liquid Crystals. *Molecular Crystals and Liquid Crystals* **2012**, *557*(1), 50–59.
42. Wang, M.; He, L.; Zorba, S.; Yin, Y. Magnetically Actuated Liquid Crystals. *Nano Letters* **2014**, *14*(7), 3966–3971.
43. Erb, R. M.; Martin, J. J.; Soheilian, R.; Pan, C.; Barber, J. R. Actuating Soft Matter with Magnetic Torque. *Advanced Functional Materials* **2016**, *26*(22), 3859–3880.
44. Tomašovičová, N.; Timko, M.; Mitróová, Z.; Koneracká, M.; Rajňak, M.; Éber, N.; Tóth-Katona, T.; Chaud, X.; Jadzyn, J.; Kopčanský, P. Capacitance Changes in Ferronematic Liquid Crystals Induced by Low Magnetic Fields. *Physical Review E* **2013**, *87*(1), 014501.
45. Kopčanský, P.; Tomašovičová, N.; Koneracká, M.; Timko, M.; Závišová, V.; Éber, N.; Fodor-Csorba, K.; Tóth-Katona, T.; Vajda, A.; Jadzyn, J.; Beaugnon, E.; Chaud, X. The Structural Instabilities in Ferronematic Based on Liquid Crystal with Negative Diamagnetic Susceptibility Anisotropy. *Journal of Magnetism and Magnetic Materials* **2010**, *322*(22), 3696–3700.
46. Kopčanský, P.; Koneracká, M.; Timko, M.; Jadzyn, J. The Study of Structural Transitions in Liquid Crystal Droplets Doped with Magnetic Particles. *physica status solidi (b)* **2006**, *243*(1), 317–321.

47. Tomašovičová, N.; Timko, M.; Mitróová, Z.; Koneracká, M.; Rajňak, M.; Éber, N.; Tóth-Katona, T.; Chaud, X.; Jadzyn, J.; Kopčanský, P. Capacitance Changes in Ferronematic Liquid Crystals Induced by Low Magnetic Fields. *Physical Review E* **2013**, *87*(1), 014501.
48. Mikelson, A.; Karklin, Y. Control of Crystallization Processes by Means of Magnetic Fields. *Journal of Crystal Growth* **1981**, *52*, 524–529.
49. *Materials science in static high magnetic fields*; Watanabe, K., Motokawa, M., Eds.; Springer:, **2013**.
50. Yin, D. C.; Protein crystallization in a magnetic field. *Progress in Crystal Growth and Characterization of Materials* **2015**, 61(1), 1-26.
51. Onodera, R.; Kimura, S.; Watanabe, K.; Yokoyama, Y.; Makino, A.; Koyama, K. Isothermal Crystallization of Iron-Based Amorphous Alloys in a High Magnetic Field. *Materials Transactions* **2013**, *54*(7), 1232–1235.
52. Chandrasekhar, R. Influence of Magnetic Field on Sodium Hexafluorosilicate Synthesis. *Journal of Crystal Growth* **2000**, *216*(1-4), 407–412.
53. Sepehri-Amin, H.; Hirosawa, S.; Hono, K. Advances in Nd-Fe-B Based Permanent Magnets. *Handbook of Magnetic Materials* **2018**, 269–372.
54. Rucman., S.; Jakmunee, J.; Punyodom, W.; Singjai, P. A Novel Strategy for Longevity Prolongation of Iron-Based Nanoparticle Thin Films by Applied Magnetic Force. New Journal of Chemistry 2018, 42 (7), 4807–4810.
55. Ručman, S.S.; Punyodom, W.; Jakmunee, J.; Singjai, P. Inducing Crystallinity of Metal Thin Films with Weak Magnetic Fields without Thermal Annealing. *Crystals* **2018**, 8, 362.
56. Tai, C. Y.; Wu, C.-K.; Chang, M.-C. Effects of Magnetic Field on the Crystallization of $CaCO_3$ Using Permanent Magnets. *Chemical Engineering Science***2008**, *63*(23), 5606–5612.
57. Cefalas, A.; Kobe, S.; Dražic, G.; Sarantopoulou, E.; Kollia, Z.; Stražišar, J.; Meden, A. Nanocrystallization of $CaCO_3$ at Solid/Liquid Interfaces in Magnetic Field: A Quantum Approach. *Applied Surface Science* **2008**, *254*(21), 6715–6724.
58. Mitrović, M. Growth Rate Dispersion of Small $MnCl_2 \cdot 4H_2O$ Crystals II. Growth in a Magnetic Field. *Journal of Crystal Growth* **1991**, *112*(1), 171–182.

59. Mitrović, M.; Žižić, B.; Napijalo, M. Influence of Magnetic Field on Growth Rate Dispersion of Small Rochelle Salt Crystals. *Journal of Crystal Growth* **1988**, *87*(4), 439–445.
60. Mitrović, M. M.; Ristić, R. I.; Ćirić, I. The Influence of a Magnetic Field on the Mosaic Spread and Growth Rate of Small Rochelle Salt Crystals. *Applied Physics A Solids and Surfaces* **1990**, *51*(5), 374–378.
61. Coey, J. M. D.; Cass, S. Magnetic Water Treatment. *Journal of Magnetism and Magnetic materials* **2000**, *209*(1-3), 71-74.
62. Ohgaki, K.; Makihara, Y.; Sangawa, H. Effect of Exposure to Magnetism on Crystals Produced in Aqueous Solutions. *Chemical Engineering Science* **1994**, *49*(6), 911–913.
63. Madsen, H. Influence of Magnetic Field on the Precipitation of Some Inorganic Salts. *Journal of Crystal Growth* **1995**, *152*(1-2), 94–100.
64. Fan, P.; Jiang, X.; Qiao, J.; Li, L. Enhanced Removal of Heavy Metals by Zerovalent Iron in Designed Magnetic Reactors. *Environmental Technology* **2017**, *39*(19), 2542–2550.
65. Liang, L.; Guan, X.; Shi, Z.; Li, J.; Wu, Y.; Tratnyek, P. G. Coupled Effects of Aging and Weak Magnetic Fields on Sequestration of Selenite by Zero-Valent Iron. *Environmental Science & Technology* **2014**, *48*(11), 6326–6334.
66. Xu, C.; Zhang, B.; Zhu, L.; Lin, S.; Sun, X.; Jiang, Z.; Tratnyek, P. G. Sequestration of Antimonite by Zerovalent Iron: Using Weak Magnetic Field Effects to Enhance Performance and Characterize Reaction Mechanisms. *Environmental Science & Technology* **2016**, *50*(3), 1483–1491.
67. Fan, P.; Sun, Y.; Qiao, J.; Lo, I. M.; Guan, X. Influence of Weak Magnetic Field and Tartrate on the Oxidation and Sequestration of Sb(III) by Zerovalent Iron: Batch and Semi-Continuous Flow Study. *Journal of Hazardous Materials* **2018**, *343*, 266–275.
68. Li, J.; Qin, H.; Zhang, W.-X.; Shi, Z.; Zhao, D.; Guan, X. Enhanced Cr(VI) Removal by Zero-Valent Iron Coupled with Weak Magnetic Field: Role of Magnetic Gradient Force. *Separation and Purification Technology* **2017**, *176*, 40–47.

69. Saban, K.; Jini, T.; Varghese, G. Influence of Magnetic Field on the Growth and Properties of Calcium Tartrate Crystals. *Journal of Magnetism and Magnetic Materials* **2003**, *265*(3), 296–304.
70. Sazaki, G.; Durbin, S. D.; Miyashita, S.; Ujihara, T.; Nakajima, K.; Motokawa, M. Magnetic Damping of the Temperature-Driven Convection in NaCl Aqueous Solution Using a Static and Homogeneous Field of 10 T. *Japanese Journal of Applied Physics* **1999**, *38*(Part 2, No. 7B). 842-844
71. Wang, Z.; Xu, H.; Ni, J.; Li, Q.; Zhou, B. Effect of High Magnetic Field on the Crystallization of $Nd_2Fe_{14}B$/α-Fe Nanocomposite Magnets. *Rare Metals* **2006**, *25*(4), 337–341.
72. Wang, Z.; Liu, W.; Zhou, B.; Ni, J.; Xu, H.; Li, Q. Microstructural Characteristics of $Nd_2Fe_{14}B$/α-Fe Nanocomposite Ribbons Bearing Nb Element. *Rare Metals* **2008**, *27*(3), 299–302.
73. Zhuang, Y.; Chen, J.; Liu, W.; He, J. Effect of High Magnetic Field on Crystallization of Zr46.75Ti8.25Cu7.5Ni10Be27.5 Bulk Metallic Glass. *Journal of Alloys and Compounds* **2010**, *504S*. 256-259.
74. Madsen, H. E. L. Theory of Electrolyte Crystallization in Magnetic Field. *Journal of Crystal Growth* **2007**, *305*(1), 271–277.
75. Coey, J.M.D.; Magnetic Water Treatment–How Might it Work?. *Philosophical Magazine* **2012**, 92, 3857-3865.
76. Powell, M. R.; Magnetic Water and Fuel Treatment: Myth, Magic, or Mainstream Science?. *Skeptical Inquirer* **1998**, 22.1, 27-31.
77. Swann, S.; Magnetron Sputtering. *Physics in Technology* **1988**, 19, 67-75.
78. Quintero, J.; Mariño, A.; Šiller, L.; Restrepo-Parra, E.; Caro-Lopera, F. Rocking Curves of Gold Nitride Species Prepared by Arc Pulsed - Physical Assisted Plasma Vapor Deposition. *Surface and Coatings Technology* **2017**, *309*, 249–257.
79. Matsuda, T.; Umeda, K.; Kato, Y.; Nishimoto, D.; Furuta, M.; Kimura, M. Rare-Metal-Free High-Performance Ga-Sn-O Thin Film Transistor. *Scientific Reports* **2017**, *7*(1). 44326-44332.
80. Sudha, C.; Sivanarendiran, R.; Srinivasan, K. Influence of Magnetic Field on the Nucleation Rate Control of Mono Paracetamol. *Crystal Research and Technology***2015**, *50*(3), 230–235.

81. Koker, N. D.; Steinle-Neumann, G.; Vlcek, V. Electrical Resistivity and Thermal Conductivity of Liquid Fe Alloys at High P and T, and Heat Flux in Earths Core. *Proceedings of the National Academy of Sciences* **2012**, *109*(11), 4070–4073.
82. Reference Data for the Density and Viscosity of Liquid Aluminum and Liquid Iron. *Chemistry International -- Newsmagazine for IUPAC* **2006**, *28*(3).
83. Mu, Y.; Jia, F.; Ai, Z.; Zhang, L. Iron Oxide Shell Mediated Environmental Remediation Properties of Nano Zero-Valent Iron. *Environmental Science: Nano* **2017**, *4*(1), 27–45.
84. Li, H.-H.; Fu, Q.-Q.; Xu, L.; Ma, S.-Y.; Zheng, Y.-R.; Liu, X.-J.; Yu, S.-H. Highly Crystalline PtCu Nanotubes with Three Dimensional Molecular Accessible and Restructured Surface for Efficient Catalysis. *Energy & Environmental Science* **2017**, *10*(8), 1751–1756.
85. Electric glow discharge, Basic Glow Discharge Structure accessed from https://www.plasma-universe.com/Electric_glow_discharge
86. Fujita, H.; Kouno, T.; Noguchi, Y.; Ueguri, S. Breakdown Voltages of Gaseous N_2 and Air from Normal to Cryogenic Temperatures. *Cryogenics* **1978**, *18*(4), 195–200.
87. Wang, X.; Zheng, W.; Tian, H.; Yu, S.; Xu, W.; Meng, S.; He, X.; Han, J.; Sun, C.; Tay, B. Growth, Structural, and Magnetic Properties of Iron Nitride Thin Films Deposited by Dc Magnetron Sputtering. *Applied Surface Science* **2003**, *220*(1-4), 30–39.
88. Khan, W.; Wang, Q.; Jin, X.; Feng, T. The Effect of Sputtering Parameters and Doping of Copper on Surface Free Energy and Magnetic Properties of Iron and Iron Nitride Nano Thin Films on Polymer Substrate. *Materials* **2017**, *10*(2), 217.